Article

Research on Influencing Factors of Load Capacity of Pneumatic Actuator

Yisi Liu and Hanlin Sheng *

Article

Research on Influencing Factors of Load Capacity of Pneumatic Actuator

Yisi Liu [1] and Hanlin Sheng [2],*

[1] College of Aerospace Engineering, Nanjing University of Aeronautics and Astronautics; yssz182111214@nuaa.edu.cn

[2] College of Energy and Power Engineering, Nanjing University of Aeronautics and Astronautics; dreamshl@nuaa.edu.cn

* Correspondence: dreamshl@nuaa.edu.cn

Abstract: In order to solve the shortcomings of poor adaptability of traditional rigid gripper, soft robot comes into being. As the most important component of soft robot, the pneumatic actuator can drive robot movement. However, the effect of the actuator pneumatic network geometry on the actuator load capacity is insufficient. In this paper, the finite element analysis method is applied to calculate the load force and stability torque of the pneumatic actuator under a wide range of length and height dimensions of the pneumatic network. The effect of the network size on the structure rigidity, load capacity and deformation of the actuator is analyzed. Based on the calculation results, the effect of network structure size on the deformation and load capacity is analyzed, and the optimal geometric results with the maximum load capacity are obtained. This study provides theoretical guidance for the structural design and optimization of the pneumatic actuator.

Keywords: soft robots; pneumatic network; load capacity; deformation strategies

Introduction

Soft robot [1,2] is a new kind of soft robot designed based on natural creatures, such as fish [3], starfish [4] and octopus [5]. Compared with traditional rigid grippers, soft robot based on bionics has gradually attracted attention due to its unique safety and adaptability. Due to the highly nonlinear characteristics of its super elastic materials, soft robots are capable of adapting to various unstructured environments and offer improved safety with humans. They have been widely applied in different fields such as healthcare, services and intelligence.

The software actuator can drive the robot's movement and is the core component , [6,7] of the robot. At present, the common driving methods include intelligent material actuator [8], chemical actuator [9], wire actuator [10] and pneumatic actuator [11]. Compared with other forms of actuator, pneumatic actuators have the advantages of easy access to pneumatic source (air), no pollution, simple principle, timely response and high controllability, which has become a research hot spot in recent years. The pneumatic actuator includes fiber reinforced actuator [12], pneumatic mesh actuator [13] and multi-cavity actuator [14]. The pneumatic mesh actuator has become the focus of research in recent years because of its simple structure, deformation characteristic based on single actuator and [15] bidirectional bending motion.

Chen et al. [16,17] designed a pneumatic network actuator based on honeycomb structure, which derived from the current pneumatic actuator structure, and studied the control strategy and motion trajectory of the new actuator. Fan et al. [18] established and verified the bending angle prediction model for the pneumatic network actuator and studied the effects of the structural parameters of the pneumatic network and the driving pressure level on the bending angle in detail. Xu and Su et al [19] used simulation, theoretical model and experiment methods to study the influence of driving air pressure level on bending angle and stress distribution of the actuator and proved the accuracy of the static modeling method. In addition, the contact prediction model [20] of adjacent network of the actuator and the motion characteristics [21] of the actuator were also studied.

Based on the review of previous studies, it has been found that although many studies have been carried out on pneumatic actuator, most of the research focuses on the actuator's control strategies, theoretical prediction model and the influence of various factors on the bending angle of the actuators. The impact of the pneumatic network actuator geometry on the load capacity is not deep enough, and the load capacity is the most important performance parameter of the actuator. In this study, the finite element simulation method is used to deeply analyze the influence of the height factor and the length factor of the pneumatic network on the load capacity, which provides a reference for the structural optimization design and performance improvement of similar pneumatic actuator.

1. Numerical calculation method

1.1. Calculation model and working condition

Previous studies on the shape of pneumatic network have confirmed that rectangular network actuators are not only easy to design and process, but also require less driving pressure and have good bending and response characteristics [15]. In this study, the rectangular network is selected as the research object. The structure and parameters of the calculation model are shown in Figure 1. The actuator consists of an upper actuator layer and a bottom layer. The upper actuator layer consists of a number of discrete individual actuators arranged in a linear manner. The air sacs are connected by a bottom airway. In the figure , K is a half of the depth of the actuator (Z direction) , L is the length of a single actuator unit (X direction) , L_1 is the outer length of the actuator unit , L_2 is the gap between adjacent actuators , L_3 is the internal length of the actuator unit , H is the total height of a single actuator unit (Y direction) , H_1 is the height of the underlying material , H_2 is the height from the top of the airway to the outside top surface , H_3 is the relative height of the outside top surface of the actuator unit , H_4 is the height of the airway , and H_5 is the height from the limiting layer to the outside top surface . In this study, K = 15mm and H = 30mm remained unchanged, and changes in L, L_1、 L_3、 H_1、 H_3 and H_4 explored the impact of the structure of the actuator on the load capacity. Table 1 is the simulation calculation variable table, and the structural parameters of the actuator are processed without dimension. The table shows the variation range of each variable in this study, as well as the reference value maintained by each variable when other variables change.
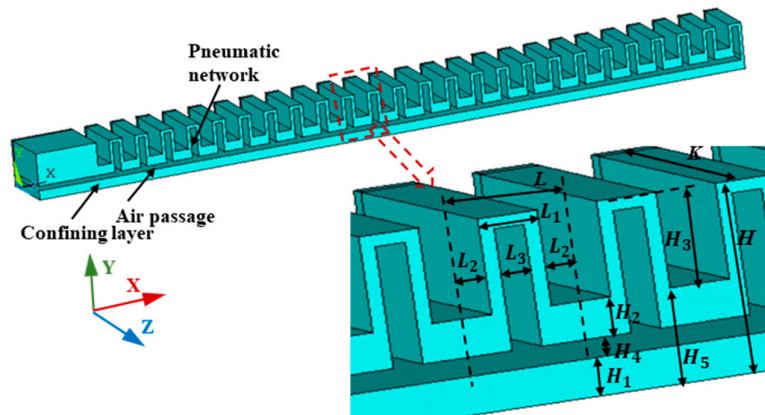

Figure 1. Schematic diagram of the structure of the calculation model.

Table 1. Simulation calculation variable table.

Variable parameters	Variable value range	Base value
Actuator unit dimensionless length L / H	0.3 ~ 1.25	0.5
The outer side of the actuator has no dimensional length L_1 / L	0.2 ~ 0.9	0.5

No dimensional length L_3 / L inside the actuator	0.2 ~ 0.8	0.5
The outer top surface of the actuator has an infinite relative height H_3 / H	0.2 ~ 0.8	0.5
Actuator airway dimensionless height H_4 / H_5	0.1 ~ 0.4	0.5
Actuator bottom layer dimensionless height H_1 / H_5	0.2 ~ 0.6	$H_1 / H_2 = 1$

1.2. Calculation method

In this study, an actuator was first drawn by SolidWorks modeling according to the calculation model and simulation calculation variable table for understanding in ANSYS modeling. An actuator unit was first drawn, and then linear array extension was carried out. Finally, the two ends were sealed or reinforced. L_2 was eliminated on both sides; The free end balloon wall extends along the Y direction to seal the airway. The fixed end of the airbag wall extends in the X direction, thickening and strengthening. ANSYS software is applied in this paper, and APDL language is used for modeling. Because of the symmetry of the model, half model is established in order to save calculational work, and tetrahedral mesh is used to divide the whole calculation model. According to the calculation of mesh convergence, the mesh size is chosen to be 1mm, and the number of model grids is about 1.58 million. The grid is shown in Figure 2.
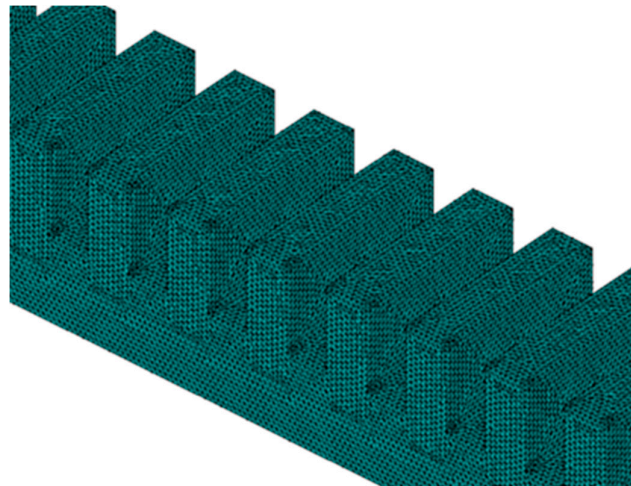

Figure 2. Finite element discretization of software actuator.

This paper mainly studies the influence of structural parameters of software actuator on load capacity. Load capacity is defined as the maximum stabilizing torque of the software actuator end when the end of the software actuator and the root are at the same height. The fixed end of the actuator is set to a fixed constraint and the symmetrical surface applies a symmetric constraint. The actuator end constraint height direction displacement. A uniform pressure load is applied to the inside of the actuator to inflate the model gas pipe, and the pressure is set to 1kPa. The application of boundary conditions is shown in Figure 3.
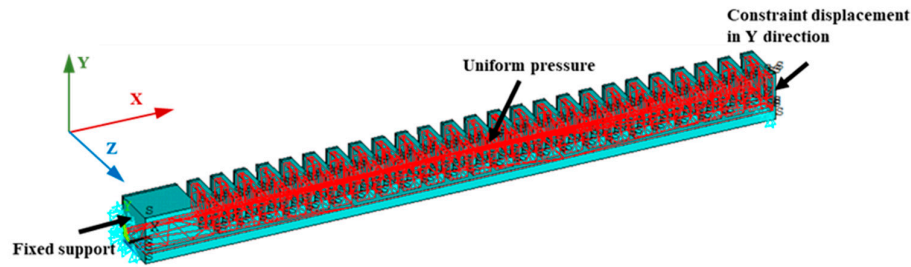
Figure 3. Application of boundary conditions.

The drive material is set as silicone material. Silicone material is a soft material, elongation in 500% ~ 1000%, with good tensile properties [22]. As can be found at the Figure 4 below, the silicone material is not a linear material, but when the tensile rate is less than 100%, the stress-tensile curve can be approximated as a linear relationship.
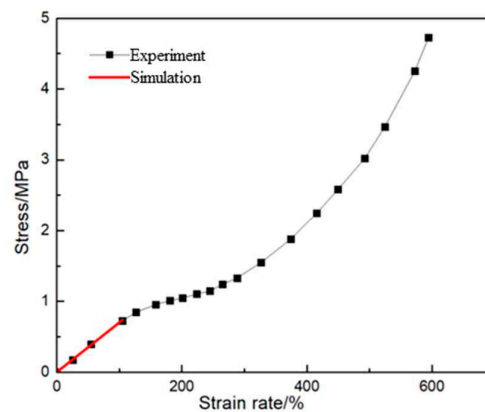

Figure 4. stress-tensile curve of silica gel material.

Due to the restriction of the end position shift, the deformation of the software actuator is small, which can be regarded as the linear elastic state. Therefore, the silica gel material can adopt the linear elastic constitutive, and the elastic modulus is E = 1MPa, μ = 0.49 [18] . The strain cloud diagram of the software actuator is shown in Figure 5, and the maximum elastic strain is 0.07. It can be seen that the silica gel material is still in the elastic stage.
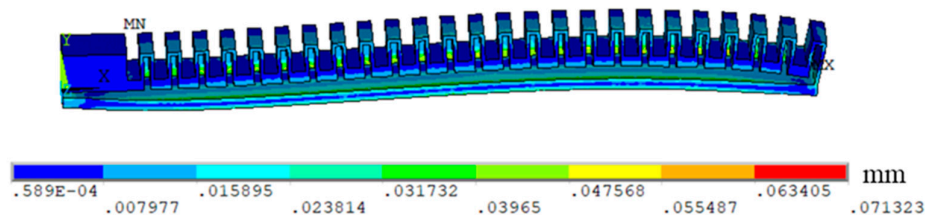

Figure 5. Strain cloud diagram of the software actuator.

1.3. Verification of calculation method

In order to verify the accuracy of the simulation model , a model consistent with previous experimental studies [15,18] was established , where L_1 = 8mm , L_2 = 1mm , L_3 = 4mm , L = 10mm , H_1 = 2mm , H_2 = 1mm , H_4 = 1mm , H_5 = 4mm , H_3 = 12mm , H = 16mm , and the number of actuator units N = 9 . Yeoh super elastic material constitutive model was adopted for the material model. The material parameters were set as C_2 = 0.094MPa, C = 0.015, and 4kPa uniform pressure was applied in the actuator. The deformation of simulation results and test results is shown in the Figure 6 below. The maximum error of the free end of the actuator is about 5mm, and the relative error is 12.8%. The

simulation results are basically consistent with the test, which indicates that the simulation results in this study are reliable.
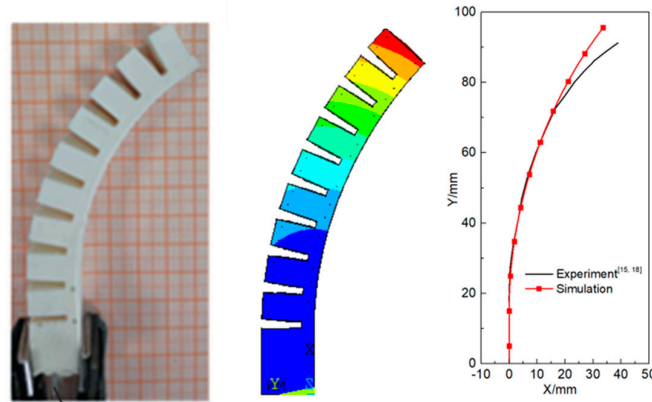

Figure 6. Comparison between simulation calculation and experimental results.

2. Results and discussion

This section discusses the effect of actuator geometry on load capacity by analyzing the most important length and width factors of the actuator.

2.1. Influence of actuator length factor on load capacity

The influence of the actuator network unit length on L and the total actuator length L_{total} on the load capacity is shown in Figure 7. Set the ratio L / H to gradually increase from 0.3 to 1.25 and study the change of load force and steady torque with L_{total} . When L_{total} is unchanged, the load capacity of the actuator does not change monotonously with L, and the load capacity is optimized under the geometric structure L / H = 0.4. In other working conditions, the load capacity increases with the increase of L_{total} (the number of network N increases). L can be reasonably designed according to the simulation results to obtain the optimal load capacity. When L is constant, the load force of the drive decreases with the increase of L_{total} , and the steady torque fluctuates with the increase of L_{total} , but the overall trend is decreasing. This is because in the case of constant input pressure, with the increase of L_{total} , the stability of the drive decreases, L_{total} resulting in a decrease in load capacity. It can be concluded that in the case of similar overall structure, the load capacity (load force and steady torque) of the driver is mainly affected by ratio L / H, and L_{total} has a great influence on load force and almost no influence on stable moment.
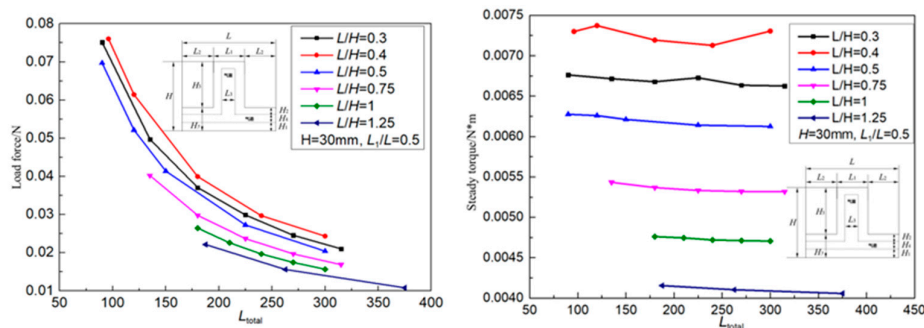

Figure 7. How the load capacity of the actuator varies with L_{total} and L.

The variation of the actuator load capacity with the outer length L_1 of the actuator is shown in Figure 8. Set L = 15mm, L_3 / L_1 = 0.5 and N = 25 unchanged and study the change of load force and steady torque with ratio L_1 / L. When the total length L of the actuator unit remains unchanged and the outer length L_1 of the actuator increases, the load capacity of the actuator continues to decrease,

with a reduction ratio of 29% . This is because with the increase of L_1 the wall thickness ($0.5 * (L_1 - L_3)$) in the direction of the length of the actuator increases and the spacing of the actuator decreases, which will increase the rigidity of the actuator, resulting in the reduction of its deformability and ultimately the load capacity. The load capacity of the actuator as the outer length L_1 of the actuator changes is shown in Figure 9. As can be seen from Figure 9, the maximum deformation of the actuator is 87mm when $L_1 / L = 0.3$, and 45mm when $L_1 / L = 0.8$. The deformation decreases as ratio L_1 / L increases, which further verifies that the rigidity of the actuator increases with the increase of ratio L_1 / L.
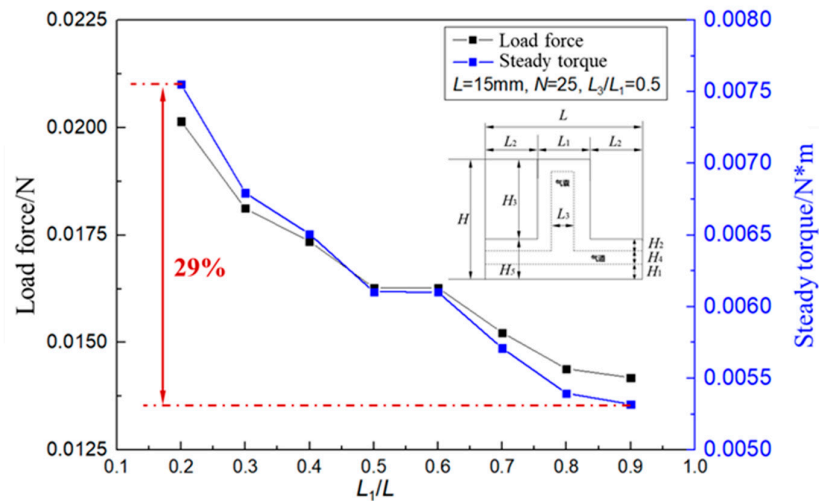

Figure 8. The load capacity of the actuator changes with the outer length L_1 of the actuator.

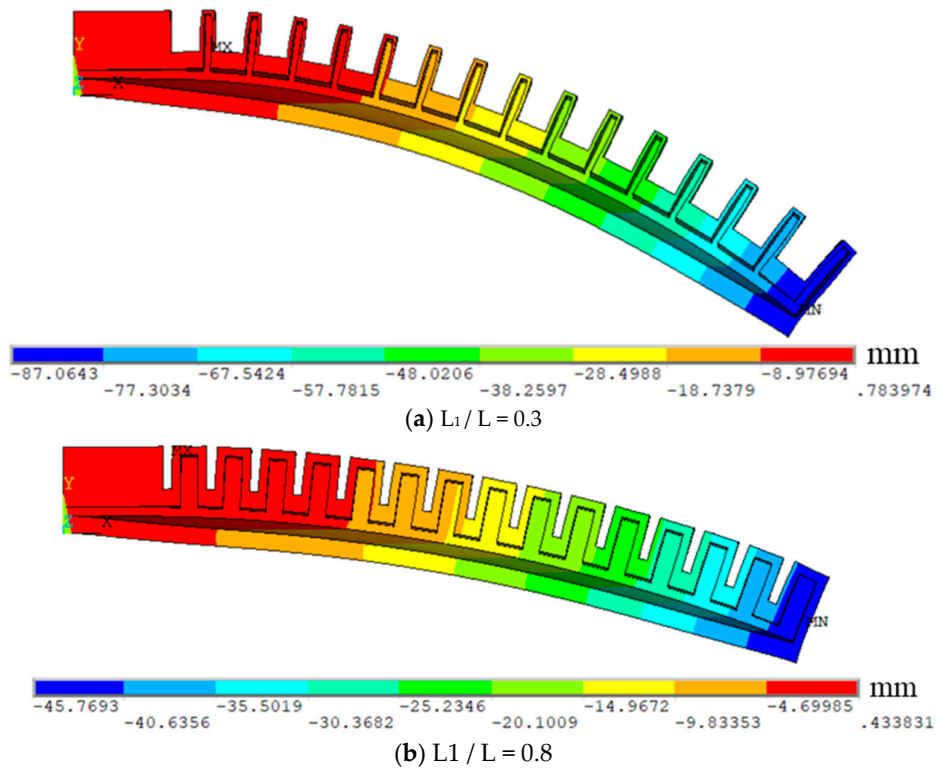(**a**) $L_1 / L = 0.3$

(**b**) $L1 / L = 0.8$

Figure 9. Actuator deformation with the outer length L_1 of the actuator.

The load capacity with the inner length L_3 of the actuator is shown in Figure 10. Set L = 15mm, L_1 / L = 0.5 and N = 25 unchanged and study the change of load force and steady torque with ratio L_3 / L. When the outer length of the actuator L_1 remains unchanged, the thickness of the actuator in the direction of length (0.5 * ($L_1 - L_3$)) decreases with the increase of L_3 , the actuator interval spacing L_2 remained unchanged, the stiffness of the actuator decreases, and the deformability of the actuator increases. The deformation change of the actuator with the inner length L_3 of the actuator is shown in Figure 11. When L_3 / L_1 = 0.3, the maximum deformation of the drive is 48mm, and when L_3 / L_1 = 0.8, the maximum deformation of the actuator is 136mm. The load capacity of the corresponding driving force is increased, and the increase range reaches 46%. The deformation increases with the increase of L_3 / L_1 , which further verifies that the drive rigidity decreases with the increase of ratio L_3 / L_1 , resulting in the increase of deformation with the increase of ratio L_3 / L_1 .
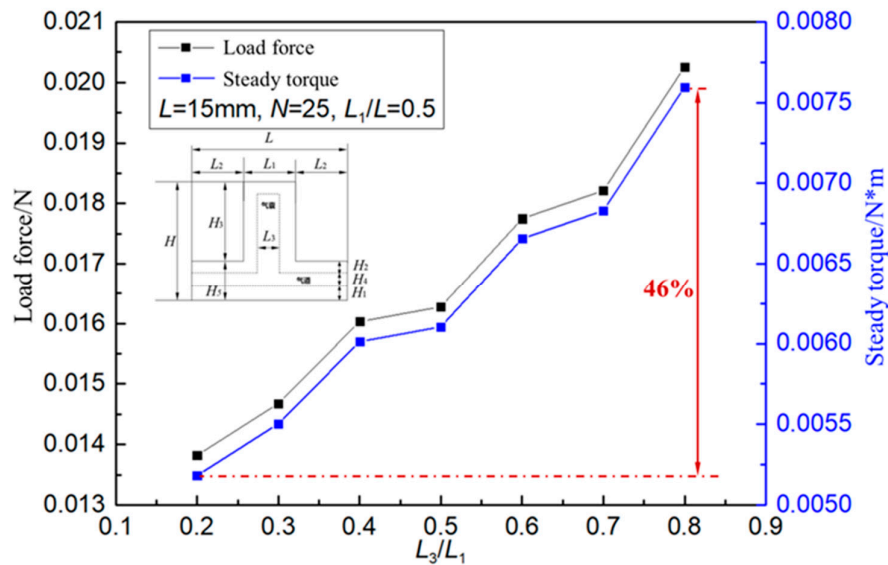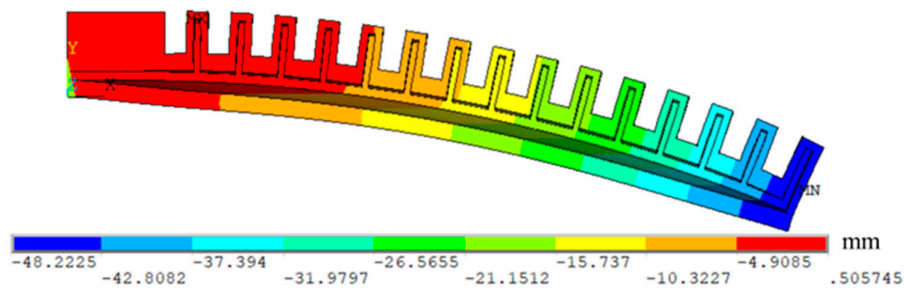

Figure 10. The load capacity of the actuator varies with the length L_3 inside the actuator.

(**a**) L3 / L1 = 0.3
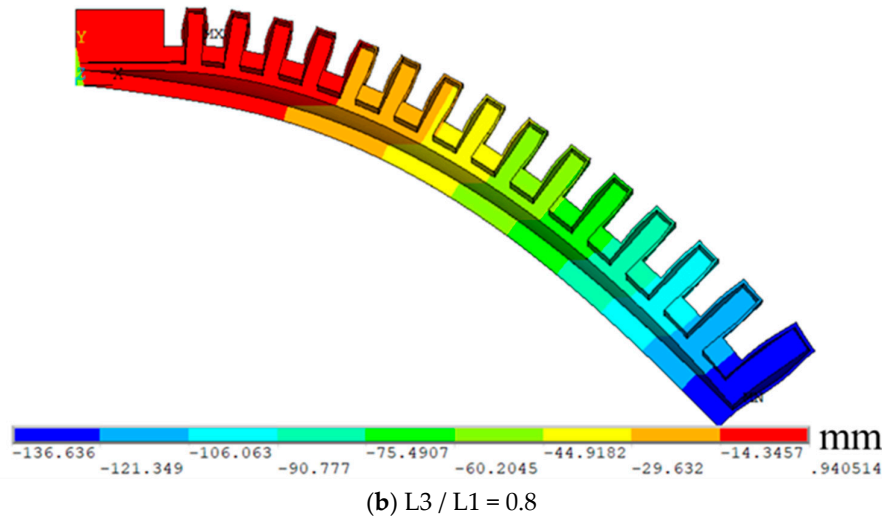
8

(**b**) L3 / L1 = 0.8

Figure 11. Change of actuator deformation with outer length L₃ of actuator.

2.2. Influence of actuator height factor on load capacity

The influence of the actuator load capacity on the relative height H_3 of the outer top surface of the actuator is shown in Figure 12. Set $H_2 = H = 30$mm and $H_4 / H = 0.1$ unchanged and study the change of load force and steady torque with H_3 / H . The variation of load force with H is complex. With the increase of H_3 the load capacity increases first and then decreases, and the load capacity reaches the maximum value under the condition of $H_3 / H = 0.5$. When the ratio H_3 / H increases to 0.5 initially ($H_3 / H = 0.2 \sim 0.5$) , the size of the actuator unit increases, the stiffness of the actuator decreases, the deformability of the actuator increases, and the load capacity increases. However, when the ratio H_3 / H continues to increase ($H_3 / H = 0.5 \sim 0.8$) , the actuator is just too low, and the grasping stability decreases, resulting in the load capacity of the actuator is reduced. The change of drive deformation with H_3 is shown in Figure 13 . Figure 13 verifies that the deformation of the drive increases monotonically with the increase of ratio H_3 / H , and the nonlinear change of the load capacity of the drive is caused by the low stiffness. In the subsequent drive structure design, it is necessary to design H to get the optimal design scheme.
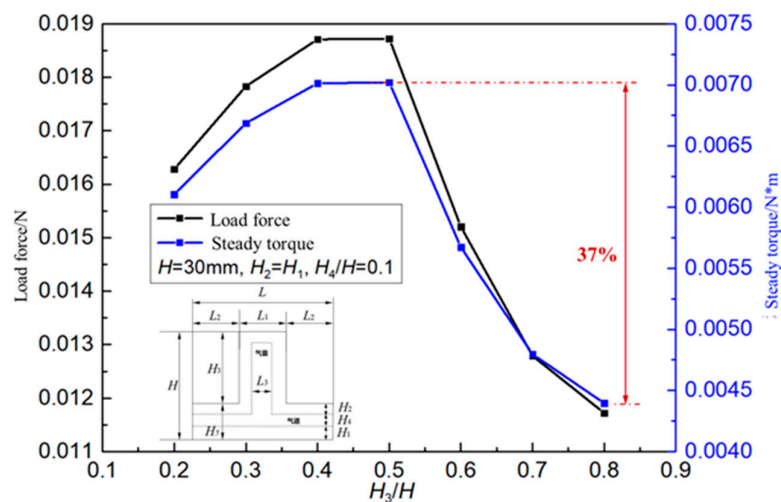

Figure 12. The load capacity of the actuator varies with the relative height H_3 of the outer top surface of the actuator.

(**a**) H3 / H = 0.2
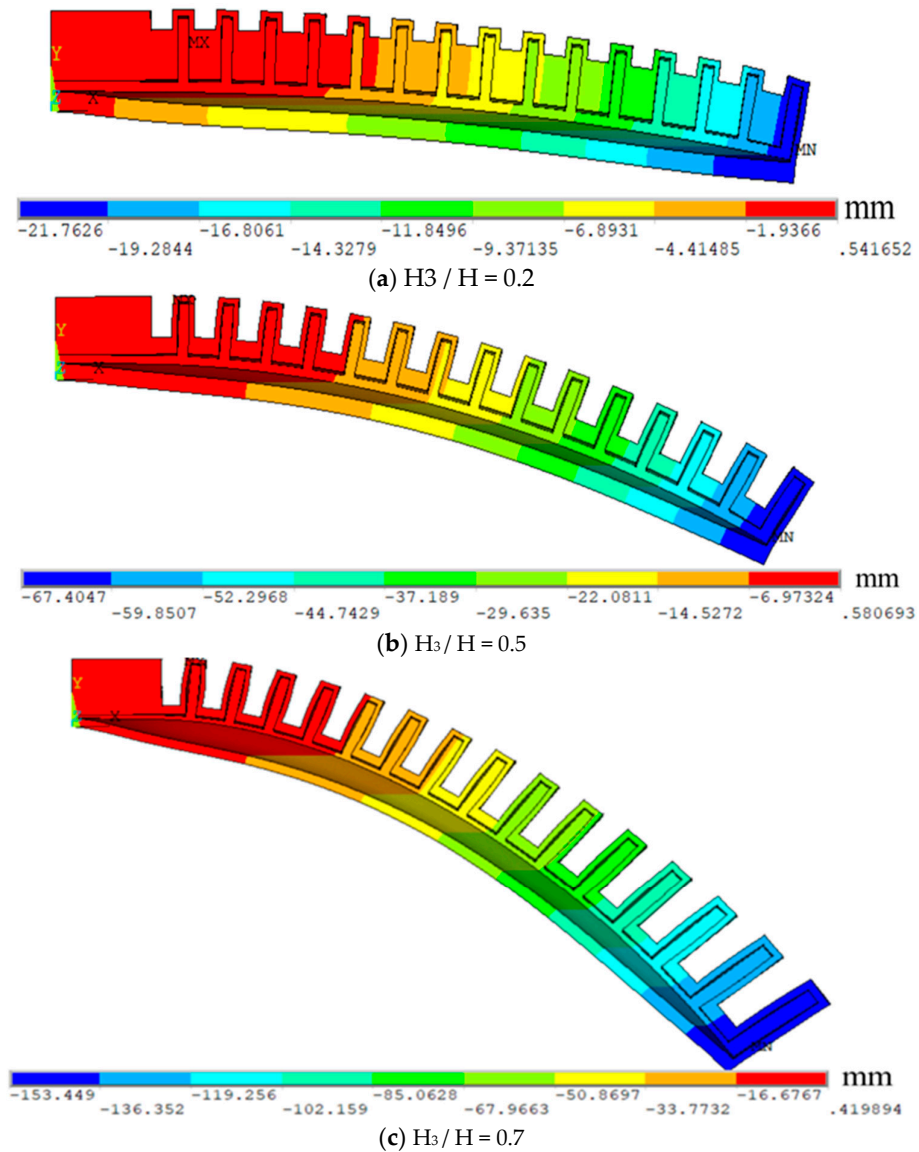
(**b**) H$_3$ / H = 0.5

(**c**) H$_3$ / H = 0.7

Figure 13. The change of actuator deformation with the relative height H$_3$ of the outer top surface of the actuator.

The variation of actuator load capacity with actuator airway height H$_4$ is shown in Figure 14. When the ratio H$_5$ / H = 0.5 is constant, the load force load capacity decreases slightly with the increase of H$_4$, and the variation range is only 6.5%. This shows that the driving force load capacity is basically not affected by the actuator airway height H$_4$.
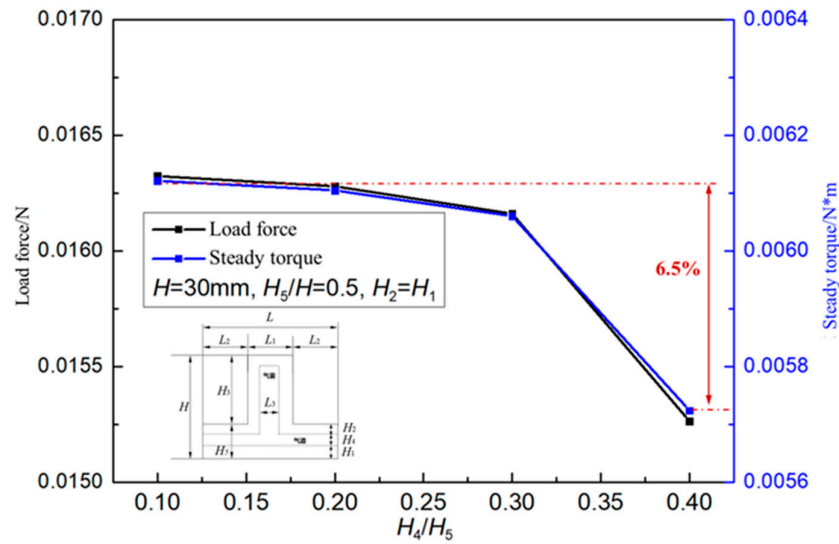
Figure 14. How the load capacity of the actuator changes with the height of the actuator airway H_4.

The actuator load capacity changes with the height H_1 of the underlying material of the actuator as shown below. When H_5 and H_4 are fixed, the underlying material H_1 increases the actuator load variation range by only 2% . This is due to the fact that while increasing H_1 will increase the drive stiffness, it will lead to a reduction in the load capacity. However, the decrease of H_2 in the process will make the driver more prone to deformability. The two factors interact with each other and the load carrying capacity of the drive in the final position is basically unchanged.
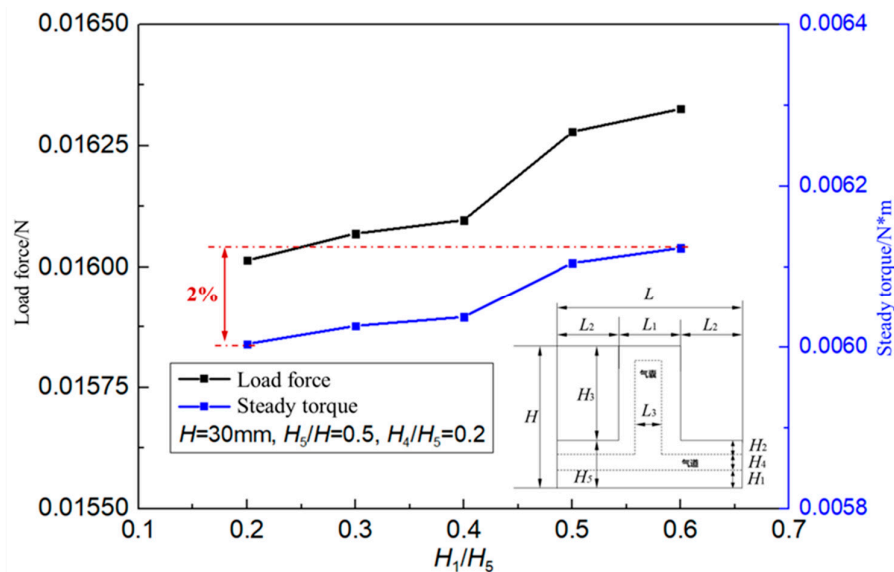

Figure 15. The load capacity of the actuator varies with the height H_1 of the underlying material of the actuator.

Conclusion

In this study, the finite element simulation method is used to study the influence of the height factor and the length factor of the soft actuator on the load capacity of the actuator, and the following conclusions are obtained:

(1) With the increase of the total length of the actuator, the actuator stability decreases, the load capacity decreases, the load capacity increases first and then decreases with the length of the actuator unit, and there is an optimal load capacity design condition when L / H = 0.4;

(2) The load capacity of the actuator decreases with the increase of the outer length of the actuator unit, and increases with the increase of the inner length of the actuator unit;

(3) The deformation and grasping stability of the robot are affected by the relative height of the outer top surface of the actuator unit, and the optimal load capacity is obtained when $H_3 / H = 0.5$;

(4) The load capacity of the actuator is little affected by the height of the bottom layer and the height of the airway. The bottom height and the airway height can be designed according to the convenience of production when designing the soft manipulator.

References

1. Kim S , Laschi C , Trimmer B. Soft robotics : a bioinspired evolution in robotics [J]. Trends in biotechnology , 2013 , 31(5) : 287-294.
2. Rus D , Tolley M T. Design , fabrication and control of soft robots [J]. Nature , 2015 , 521(7553) : 467-475.
3. Marchese A D , Onal C D , Rus D. Autonomous soft robotic fish capable of escape maneu-vers using fluidic elastomer actuators [J]. Soft robotics , 2014 , 1(1) : 75-87.
4. Shepherd R F , Ilievski F , Choi W , et al. Multigait soft robot [J]. Proceedings of the national academy of sciences , 2011 , 108(51) : 20400-20403.
5. Cianchetti M , Calisti M , Margheri L , et al. Bioinspired locomotion and gras** in water : the soft eight-arm OCTOPUS robot [J]. Bioinspiration & biomimetics , 2015 , 10(3) : 035003.
6. Xu Fengyu , Meng Fanchang , Fan Baojie , et al. Research review on Software Robot Drive , modeling and Application [J]. Journal of Nanjing University of Posts and Telecommuni-cations : Natural Science Edition , 2019 , 39(3) : 64-75.
7. Wang Yanjie , Zhao Xin , Wang Jianfeng , et al. Research Progress of Soft Robot Drive Tech-nology [J]. Chinese Hydraulics & Pneumatics , 2023 , 46(12) : 1-11.
8. Seok S , Onal C D , Cho K J , et al. Meshworm : a peristaltic soft robot with antagonistic nickel titanium coil actuators [J]. IEEE/ASME Transactions on mechatronics , 2012 , 18(5) : 1485-1497.
9. Bartlett N W , Tolley M T , Overvelde J T B , et al. A 3D-printed , functionally graded soft ro-bot powered by combustion [J]. Science , 2015 , 349(6244) : 161-165.
10. Cianchetti M , Ranzani T , Gerboni G , et al. STIFF-FLOP surgical manipulator : Mechanical design and experimental characterization of the single module [C]//2013 IEEE/RSJ interna-tional conference on intelligent robots and systems. IEEE , 2013 : 3576-3581.
11. Marchese A D , Katzschmann R K , Rus D. Whole arm planning for a soft and highly com-pliant 2d robotic manipulator [C]//2014 IEEE/RSJ International Conference on Intelligent Robots and Systems. IEEE , 2014 : 554-560.
12. Polygerinos P , Galloway K C , Savage E , et al. Soft robotic glove for hand rehabilitation and task specific training [C]//2015 IEEE international conference on robotics and automation (ICRA). IEEE , 2015 : 2913-2919.
13. Deng M , Wang A , Wakimoto S , et al. Characteristic analysis and modeling of a miniature pneumatic curling rubber actuator [C]//The 2011 International Conference on Advanced Mechatronic Systems. IEEE , 2011 : 534-539.
14. Mosadegh B , Polygerinos P , Keplinger C , et al. Pneumatic networks for soft robotics that actuate rapidly [J]. Advanced functional materials , 2014 , 24(15) : 2163-2170.
15. Fan Yi. Research and Application of Pneumatic Mesh Software Actuator [D]. Nanjing University of Aeronautics and Astronautics , 2020.
16. Wang Ningyang , Sun Hao , Jiang Hao , et al. Research on Grasping Strategy of Software gripper based on Honeycomb Pneumatic Network [J]. Robot , 2016 , 38(3) : 371-377.
17. Jiang H , Wang Z , ** Y , et al. Hierarchical control of soft manipulators towards unstruc-tured interactions [J]. The International Journal of Robotics Research , 2021 , 40(1) : 411-434.
18. Bending Deformation Prediction Method for Pneumatic Mesh Soft Actuator [J]. ** Me-chanical Engineering , 2020 , 31(09) : 1108.
19. Su iyi , Xu Qiping , Liu Jinyang. Theoretical Modeling , Simulation Analysis and Experi-mental Research of Pneumatic toothed Software Actuator [J]. Journal of Shanghai Jiao Tong University , 2023 , 57(8) : 1016.
20. Xu Qiping , Liu Jinyang. Modeling and Simulation of multi-cavity pneumatic Soft Actuator [J]. Journal of Shanghai Jiao Tong University , 2020 , 54(6) : 551.

21. Fei Yanqiong , Pang Wu , Yu Wenbo. Research on Motion of Pneumatic Driven Soft Robot [J]. Journal of Mechanical Engineering , 2017 , 53(13) : 14-18.
22. Liu Yuchao. Research on Cavity Type Pneumatic Soft Arm [D]. Harbin Institute of Tech-nology , 2020.